A Model for the Growth of a Solid Tumor with Non-uniform Oxygen Consumption

D. L. S. McELWAIN
Department of Mathematics, University of Newcastle, New South Wales, Australia, 2308, and Department of Applied Mathematics, Research School of Physical Sciences, Australian National University, Canberra, A.C.T., Australia.

AND

P. J. PONZO
Department of Applied Mathematics, Faculty of Mathematics, University of Waterloo, Waterloo, Ontario, Canada.

Received 28 October 1976; revised 11 March 1977

ABSTRACT

A model for the growth of a solid *in vitro* tumor including the effects of non-uniformity in oxygen consumption and proliferation rate is developed. The appropriate equations which describe the diffusion of oxygen are set up and then solved. The growth equation is formulated and a method of solution described. The results of this new model are compared with the predictions of an earlier model which assumes that the consumption of nutrient by live cells is uniform.

1. INTRODUCTION

Recently Deakin [5] has extended models for the growth of a solid spherical *in vitro* tumor developed by Burton [4] and Greenspan [9]. His model included the effects of non-uniformity in the consumption of oxygen by live cells in the tumor. Deakin pointed out that there is experimental evidence [8] to show that when the oxygen concentration around a cell, which we denote by σ, falls below some critical value, $\hat{\sigma}$, say, then the oxygen consumption by the cell also falls. This decrease has been explained in terms of a simple diffusion model by Boag [2].

Deakin modeled this decrease in oxygen consumption per unit volume of the solid tumor as a linear function of the oxygen concentration σ. If σ_i is the critical oxygen concentration below which tumor cells die, then if $\sigma < \sigma_i$ the cells are dead and the oxygen consumption is zero. If σ is greater than σ_i

but less than $\hat{\sigma}$, then the rate of oxygen consumption per unit volume per unit time is $A\sigma/\hat{\sigma}$, where A is a constant. If $\sigma > \hat{\sigma}$, then this oxygen consumption rate is just a constant A per unit volume. In summary,

$$O_2 \text{ consumption} = \begin{cases} 0, & \sigma < \sigma_i, \\ \dfrac{A\sigma}{\hat{\sigma}}, & \sigma_i < \sigma < \hat{\sigma}, \\ A, & \hat{\sigma} < \sigma. \end{cases} \tag{1}$$

Whereas Deakin's work considered only the oxygen diffusion problem and the effect of the non-uniformity of consumption of oxygen on the viable rim thickness, this paper develops a model which incorporates the effect of this non-uniformity on the growth rate of a solid tumor. In the Appendix to his paper, Greenspan [9] mentions the possibility of both a non-uniform nutrient consumption rate and a non-constant proliferation rate for live cells, but does not investigate the effects of these on the growth pattern of the tumor. Recently, Greenspan [10] has generalized his model to consider the distortion of shape due to an arbitrary distribution of nutrient, but the assumptions of uniform oxygen consumption and uniform local proliferation rate are retained. In the next section the model is developed, and Sec. 3 gives the method of solution. Section 4 discusses the results and conclusions.

2. THE MODEL

There is considerable experimental evidence to show that the growth fraction in solid tumors decreases markedly as the distance from a blood supply increases (see, e.g., [6]). This phenomenon seems to be widely accepted, and it appears to be true both *in vitro* [7] and *in vivo* [1, 16]. Here we model the proliferation rate in a manner similar to that adopted by Deakin for the consumption of oxygen. We assume that if the concentration of nutrient σ, presumably oxygen (Sutherland and Durand [15]), is above the critical level $\hat{\sigma}$, the proliferation rate per unit volume is a constant, which we denote by s. If the concentration σ lies in the range $\sigma_i \leqslant \sigma \leqslant \hat{\sigma}$, then the proliferation rate per unit volume is $\sigma s/\hat{\sigma}$. If $\sigma < \sigma_i$, then the region is necrotic and the proliferation rate is zero.

One microscopic model which yields this form for the proliferation rate can be outlined as follows. We assume that the average doubling time for a cell with sufficient nutrient is t_d, but that it *increases* as the ambient nutrient concentration σ decreases below the critical value $\hat{\sigma}$. That is, if $T(\sigma)$ is the cycle time, then

$$T(\sigma) = \frac{t_d}{f(\sigma)}, \tag{2}$$

where $f(\sigma)$ equals 1 if $\sigma > \hat{\sigma}$, but $f(\sigma)$ tends to zero as σ tends to zero. We also assume that $f(\sigma)$ satisfies $0 \leqslant f(\sigma) \leqslant 1$. Further, assuming a fixed amount of nutrient Σ is required for doubling, which occurs after time $T(\sigma)$, then the average rate of absorption of nutrient by a single cell is

$$\frac{\Sigma}{T(\sigma)} \equiv \frac{\Sigma f(\sigma)}{t_d}. \tag{3}$$

If we further hypothesize that each cell occupies the same "effective" volume Δ, then a small volume element dv will contain dv/Δ cells. In a time $T(\sigma)$ these cells will double and the increase in the number of cells will also be dv/Δ, so that the average rate of increase is $dv/\Delta T(\sigma)$ cells/unit time. The total rate of increase in volume V is then

$$\frac{dN}{dt} = \iiint_V \frac{dv}{\Delta T(\sigma)}. \tag{4}$$

In terms of the volume V this equation becomes

$$\frac{dV}{dt} = \iiint_V \frac{dv}{T(\sigma)},$$

i.e.,

$$\frac{dV}{dt} = \iiint_V \frac{f(\sigma)}{t_d} dv. \tag{5}$$

If R_0 is the outer tumor radius, and we assume spherical symmetry, this becomes

$$\frac{4\pi}{3}\frac{dR_0^3}{dt} = 4\pi \int_0^{R_0} r^2 \frac{f(\sigma)}{t_d} dr$$

$$= 4\pi \int_0^{R_0} r^2 s(\sigma)\, dr, \quad \text{say,}$$

where $s(\sigma) = f(\sigma)/t_d = sf(\sigma)$ with s the "normal" proliferation rate, i.e., in the region where $f(\sigma) = 1$. If we assume a linear form for $f(\sigma)$ as was done by Deakin [5], which seems reasonable in the light of the experiments of Froese [8], then $s(\sigma)$ has the form

$$s(\sigma) = \begin{cases} 0, & \sigma < \sigma_i, \\ \dfrac{s\sigma}{\hat{\sigma}}, & \sigma_i < \sigma < \hat{\sigma}, \\ s, & \hat{\sigma} < \sigma. \end{cases}$$

One obvious implication of this microscopic model is that the cycle time will increase with decreasing oxygen concentration and therefore with increasing distance from the nutrient supply. Tubiana [1] has reviewed the experimental data on cycle times in tumors, and it seems obvious that in some types of solid tumors, although the *growth fraction* decreases away from the nutrient supply, the *cycle time* remains the same throughout the viable cells. On the other hand, some workers characterize the latter stages of tumor growth, the post-exponential growth, by a lengthening of the mitotic cycle time [3,6,15].

Lala and Patt [12] and other authors have demonstrated that for an Ehrlich ascitic tumor there is a marked increase in cycle time as the tumor ages, which results in a deceleration of growth. However, Lala, in a personal communication to Tubiana [11], points out that when these were grown as spherical clones, no change in the cycle times was observed with increasing age of the tumor, although the growth fraction did decrease with age.

Whether the microscopic model developed above is valid or not, there is certainly no doubt that the growth fraction, and therefore the proliferation rate, decreases in regions where the oxygen concentration decreases. With this in mind, this paper investigates a linear relationship between the proliferation rate and oxygen concentration. We note here that Wette et al. [18] have used a very similar relationship in their stochastic model of solid tumor growth. In their paper they assume that the local birth rate and therefore also the local proliferation rate are proportional to the local nutrient concentration. We note here that another acceptable form for $s(\sigma)$ is

$$s(\sigma)=\begin{cases} 0, & \sigma<\sigma_i, \\ s\dfrac{\sigma-\sigma_i}{\hat{\sigma}-\sigma_i}, & \sigma_i<\sigma<\hat{\sigma}, \\ s, & \hat{\sigma}<\sigma. \end{cases}$$

This would mean that the local growth rate was continuous across the necrotic-core–viable-shell boundary. However, in this paper we adopt the same form for $f(\sigma)$ used by Deakin [5].

We characterize the growth pattern as follows.

2.1. *PHASE I*

During the first stage of growth all cells obtain sufficient oxygen, that is, the condition $\sigma>\hat{\sigma}$ holds everywhere and mitosis proceeds normally, all cells consuming oxygen at a uniform rate. This period of growth is exponential and continues until the concentration of oxygen at the center of the nodule drops to the critical value $\hat{\sigma}$.

2.2. *PHASE II*

After this time, the proliferation rate in the central portion of the tumor decreases and the overall growth rate begins to slow down. This phase continues until the oxygen concentration at the center of the tumor drops below the level necessary to support life, σ_i, and the cells begin to die, forming a coagulative necrotic core.

2.3. *PHASE III*

In this phase, the rate of growth further decreases and the tumor eventually reaches a viable dormant state with a three layer structure. In the outer shell, where $\sigma > \hat{\sigma}$, the cells behave in the same way as in the exponential phase, with normal mitosis and oxygen consumption. Inside this, there is a shell of viable cells which have an environment in which the oxygen concentration σ is in the range between σ_i and $\hat{\sigma}$. For this region the oxygen consumption and the proliferation rate are reduced below their "normal" values. The inner sphere consists of coagulative necrotic debris, and in this region the oxygen concentration is σ_i with no oxygen consumed by the cells.

This viable dormant state can only exist if there is a volume loss mechanism to balance the volume gain due to the mitotic activity in the viable regions of the tumor. Here we adopt the Greenspan hypothesis [9], although in a subsequent paper [13] we shall discuss another volume loss mechanism and its effects on the growth pattern of solid tumors. Greenspan assumes that the live cells disintegrate after being forced into the necrotic region and "degenerate into simpler permeable compounds." This leads to a volume loss term in the growth equation, with the rate of volume loss proportional to the necrotic core volume.

3. MATHEMATICS OF THE MODEL

We denote by R, $\hat{R}$ and R_i the outer radii of the spherical nodule, the region of slow growth, and the necrotic core, respectively, where we assume that the nodule is spherically symmetric. The corresponding values of the concentration σ are σ_∞, $\hat{\sigma}$ and σ_i.

3.1. *PHASE I*

In the first phase, if the assumption of diffusive equilibrium is made (see Greenspan [9] for a discussion), then the appropriate diffusion equation is

$$\frac{k}{r^2}\frac{d}{dr}\left[r^2\frac{d\sigma}{dr}\right] = A, \qquad 0 \leqslant r \leqslant R_0, \tag{6}$$

where k is the diffusion coefficient for oxygen in the tumor and A is the

normal oxygen consumption rate. The solution to this equation subject to the appropriate boundary condition is

$$\sigma(r) = \sigma_\infty + \frac{A}{6k}(r^2 - R_0^2). \tag{7}$$

The growth equation during this phase of the growth is

$$\frac{4\pi}{3}\frac{dR_0^3}{dt} = s \cdot \frac{4\pi}{3} R_0^3. \tag{8}$$

If we introduce a scaled time τ as $\tau = st$, then integration of Eq. (8) gives

$$R_0(\tau) = R_0(0)e^{\tau/3}, \tag{9}$$

where $R_0(0)$ is the initial tumor radius. If we also introduce a scaled radius in the form $\xi = BR_0$, where $B = (A/k\hat{\sigma})^{1/2}$, then this equation becomes

$$\xi(\tau) = \xi(0)e^{\tau/3}. \tag{10}$$

This exponential phase continues until $\sigma = \hat{\sigma}$ at the center of the nodule. We denote the corresponding scaled outer radius by ξ_s; it is given by

$$\xi_s = \left[6\left(\frac{\sigma_\infty}{\hat{\sigma}} - 1\right)\right]^{1/2}. \tag{11}$$

3.2. *PHASE II*

During the second phase, the diffusion of oxygen is governed by the equation

$$\frac{k}{r^2}\frac{d}{dr}\left[r^2\frac{d\sigma}{dr}\right] = \begin{cases} A\sigma/\hat{\sigma}, & 0 \leqslant r \leqslant \hat{R}, \\ A, & \hat{R} \leqslant r \leqslant R_0. \end{cases} \tag{12}$$

This diffusion equation has been considered in some detail by Rashevsky [13] when describing the diffusion of oxygen both outside and inside a single spherical cell. Integrating this equation, applying the boundary conditions at $r = \hat{R}$ and $r = R_0$, and demanding that σ be continuous gives

$$\sigma(r) = \hat{\sigma} \cdot \frac{\hat{R}}{r}\frac{\sinh Br}{\sinh B\hat{R}}, \qquad 0 \leqslant r \leqslant \hat{R}, \tag{13a}$$

and

$$\sigma(r)=\sigma_\infty+\frac{A}{6k}(r^2-R_0^2)+\left\{\hat{\sigma}-\sigma_\infty-\frac{A}{6k}(\hat{R}^2-R_0^2)\right\}\frac{\hat{R}}{r}\frac{r-R_0}{\hat{R}-R_0}$$

$$\text{for}\quad \hat{R}\leqslant r\leqslant R_0. \tag{13b}$$

We obtain an expression for $\hat{R}$ by matching $d\sigma/dr$ at $r=\hat{R}$. This gives

$$\sigma_\infty-\hat{\sigma}=\frac{A}{6k}(R_0^2-\hat{R}^2)+\left[\hat{\sigma}\hat{R}\,(B\hat{R}\coth B\hat{R}-1)-\frac{A\hat{R}^3}{3k}\right]\left[\frac{1}{\hat{R}}-\frac{1}{R_0}\right].$$

If we put $\rho=B\hat{R}$ and recall that $\xi=BR_0$, this condition becomes

$$\frac{\sigma_\infty}{\hat{\sigma}}-1=\tfrac{1}{6}(\xi^2-\rho^2)+\left[\rho(\rho\coth\rho-1)-\frac{\rho^3}{3}\right]\left[\frac{1}{\rho}-\frac{1}{\xi}\right]. \tag{14}$$

The growth equation in this phase takes the form

$$\frac{4\pi}{3}\frac{dR_0^3}{dt}=s\cdot\frac{4\pi}{3}(R_0^3-\hat{R}^3)+4\pi s\int_0^{\hat{R}}\frac{\sigma(r)}{\hat{\sigma}}r^2dr. \tag{15}$$

Performing the integration with $\sigma(r)$ given by Eq. (13a) and transforming to non-dimensional variables gives

$$\xi^2\frac{d\xi}{d\tau}=\tfrac{1}{3}(\xi^3-\rho^3)+\rho\{\rho\coth\rho-1\}. \tag{16}$$

Using Eq. (14), this equation can be rewritten as

$$\xi^2\frac{d\xi}{d\tau}=\tfrac{1}{3}\xi^3+\left\{\frac{\sigma_\infty}{\hat{\sigma}}-1-\tfrac{1}{6}(\xi^2-\rho^2)\right\}\frac{\rho\xi}{(\xi-\rho)}. \tag{17}$$

The second phase continues until $\sigma(r=0)=\sigma_i$, and this occurs when $\rho=\rho_c$, where ρ_c satisfies

$$\frac{\sigma_i}{\hat{\sigma}}=\frac{\rho_c}{\sinh\rho_c}. \tag{18}$$

The corresponding value of ξ, denoted by ξ_c—the scaled outer radius at which necrosis first occurs—is given by Eq. (14) with $\rho=\rho_c$.

3.3. *PHASE III*

During the third and final stage of the growth, the oxygen diffusion is governed by the equation

$$\frac{k}{r^2}\frac{d}{dr}\left[r^2\frac{d\sigma}{dr}\right]=\begin{cases}0, & 0\leqslant r<R_i,\\ \dfrac{A\sigma}{\hat{\sigma}}, & R_i\leqslant r\leqslant \hat{R},\\ A, & \hat{R}\leqslant r\leqslant R_0,\end{cases} \tag{19}$$

and this equation is to be solved subject to continuity conditions on σ and $d\sigma/dr$ and the boundary conditions $\sigma=\sigma_i$ at $r=R_i$, $\sigma=\hat{\sigma}$ at $r=\hat{R}$ and $\sigma=\sigma_\infty$ at $r=R_0$. Since oxygen is not consumed in the necrotic core, we also impose the condition $d\sigma/dr=0$ at $r=R_i$. Deakin [5] solves this equation, and the solution is

$$\sigma(r)=\begin{cases}\sigma_i, & 0\leqslant r\leqslant R_i,\\ \dfrac{\sigma_i}{Br}\{\sinh B(r-R_i)+BR_i\cosh B(r-R_i)\}, & R_i\leqslant r\leqslant \hat{R},\\ \sigma_\infty+\dfrac{A}{6k}(r^2-R_0^2)+F\left(\dfrac{1}{R_0}-\dfrac{1}{r}\right), & \hat{R}\leqslant r\leqslant R_0,\end{cases} \tag{20}$$

where F can be determined by the condition that $\sigma=\hat{\sigma}$ at $r=\hat{R}$. Two equations result when F is eliminated, and these in terms of the non-dimensional variables are

$$\frac{\hat{\sigma}}{\sigma_i}=\frac{1}{\rho}\{\sinh(\rho-\eta)+\eta\cosh(\rho-\eta)\} \tag{21a}$$

and

$$\frac{\sigma_\infty}{\hat{\sigma}}-1=\tfrac{1}{6}(\xi^2-\rho^2)+\left(G\rho-\frac{\rho^3}{3}\right)\left(\frac{1}{\rho}-\frac{1}{\xi}\right) \tag{21b}$$

with

$$G=\frac{\sigma_i}{\hat{\sigma}}\{\cosh(\rho-\eta)+\eta\sinh(\rho-\eta)\}-1$$

and $\eta=BR_i$. In this phase the growth equation is

$$\frac{4\pi}{3}\frac{dR_0^3}{dt}=s\cdot\frac{4\pi}{3}(R_0^3-\hat{R}^3)+4\pi s\int_{R_i}^{\hat{R}}\frac{\sigma(r)}{\hat{\sigma}}r^2\,dr-3\lambda\cdot\frac{4\pi}{3}R_i^3, \tag{22}$$

where the last term arises from the volume loss term discussed in the last section with the proportionality constant taken to be 3λ. Performing the integration and writing the resulting equation in terms of non-dimensional distances and time gives

$$\xi^2 \frac{d\xi}{d\tau} = \tfrac{1}{3}(\xi^3 - \rho^3) + \frac{\sigma_i}{\hat{\sigma}} \rho \{\cosh(\rho - \eta) + \eta \sinh(\rho - \eta)\} - \frac{\sigma_i}{\hat{\sigma}} \{\sinh(\rho - \eta) + \eta \cosh(\rho - \eta)\} - \gamma \eta^3, \tag{23}$$

where $\gamma = \lambda / s$. Using Eqs. (21a and b) this equation can be simplified to yield

$$\xi^2 \frac{d\xi}{d\tau} = \tfrac{1}{3}\xi^3 + \left\{ \frac{\sigma_\infty}{\hat{\sigma}} - 1 - \tfrac{1}{6}(\xi^2 - \rho^2) \right\} \frac{\rho \xi}{(\xi - \rho)} - \gamma \eta^3, \tag{24}$$

which is the same expression for the growth equation which describes the second phase, except for the volume loss term.

4. RESULTS AND DISCUSSION

To obtain the full growth pattern, values are first given to the ratios $\sigma_\infty / \hat{\sigma}$ and $\sigma_i / \hat{\sigma}$. We used the same values as those used by Deakin, although Deakin does not give values for $\sigma_\infty / \hat{\sigma}$ explicitly. Once these are given, the end of phase I can be determined by the condition that the outer radius reaches the value ξ_s.

The pattern for the second phase growth is obtained by integrating Eq. (17) numerically using a fourth order Runge-Kutta procedure. This integration requires a knowledge of ρ for a given value of ξ, so that Eq. (14) must be solved numerically several times during each step. This phase proceeds until $\xi = \xi_c$, the outer radius at which central necrosis first occurs. The value of ξ_c is obtained first by solving Eq. (18) numerically for ρ_c and then solving Eq. (14) numerically for ξ_c given $\sigma_\infty / \hat{\sigma}$ and ρ_c.

The third and final stage of growth is described by the differential equation (24), with γ prescribed. This equation is solved numerically, the values of ρ and η being determined by solving Eqs. (21a) and (21b) simultaneously for a given value of ξ. The integration of the differential equation was carried out until the dormant phase was obtained. The values of the scaled radii for the steady state are denoted by ξ_∞, ρ_∞ and η_∞.

Tables 1 and 2 show the values of $\sigma_\infty / \hat{\sigma}$, $\sigma_i / \hat{\sigma}$ together with the values of $\xi_s, \rho_c, \xi_c, \eta_\infty, \rho_\infty, \xi_\infty$ for two values of the volume loss parameter γ. The results in Table 1 are for $\gamma = 0.5$, and those in Table 2 for $\gamma = 0.9$. Also given in the tables are the corresponding parameter values, except for ξ_s, which has the same value for this model as obtained using Greenspan's model [9]. For a

TABLE 1

Values of the Scaled Radii at Critical Stages of the Tumor Growth with $\gamma = 0.5$ for Both This Model and the Greenspan Model

$\sigma_\infty/\hat{\sigma}$	$\sigma_i/\hat{\sigma}$	ξ_s	ρ_c	ξ_c	η_∞	ρ_∞	ξ_∞	ρ_c[a]	ξ_c[a]	η_∞[a]	ρ_∞[a]	ξ_∞[a]
1.41	0.1	1.56	4.50	4.94	6.10	9.37	9.76	2.32	2.80	2.27	3.84	4.21
5.68	0.1	5.30	4.50	7.49	12.0	15.2	17.6	2.32	5.78	8.14	9.55	11.9
53.4	0.1	17.7	4.50	18.7	33.9	37.0	47.2	2.32	17.9	29.8	31.2	41.2
8.00	10^{-6}	6.48	17.4	20.5	22.8	37.7	40.8	2.45	6.93	10.1	11.6	14.6
90.6	10^{-6}	23.2	17.4	32.8	54.0	68.7	82.0	2.45	23.3	39.3	40.8	54.2
1054.0	10^{-6}	79.5	17.4	83.8	155.0	170.0	218.0	2.45	79.5	139.0	140.0	190.0

[a]These values pertain to the Greenspan model. ξ_s is the same in both models.

TABLE 2

Values for the Scaled Radii at Critical Stages of the Tumor Growth with $\gamma = 0.9$ for Both This Model and the Greenspan model

$\sigma_\infty/\hat{\sigma}$	$\sigma_i/\hat{\sigma}$	ξ_s	ρ_c	ξ_c	η_∞	ρ_∞	ξ_∞	ρ_c[a]	ξ_c[a]	η_∞[a]	ρ_∞[a]	ξ_∞[a]
1.41	0.1	1.56	4.50	4.94	4.40	7.76	8.16	2.32	2.80	1.77	3.39	3.78
5.68	0.1	5.30	4.50	7.49	8.46	11.7	14.2	2.32	5.78	5.84	7.28	9.74
53.4	0.1	17.7	4.50	18.7	23.3	26.3	36.9	2.32	17.9	20.6	22.0	32.5
8.00	10^{-6}	6.48	17.4	20.5	16.7	31.8	34.8	2.45	6.93	7.20	8.70	11.9
90.6	10^{-6}	23.2	17.4	32.8	38.6	53.4	67.0	2.45	23.3	27.1	28.6	42.6
1054.0	10^{-6}	79.5	17.4	83.8	107.0	122.0	172.0	2.45	79.5	95.1	96.5	148.0

[a]These values pertain to the Greenspan model. ξ_s is the same for both models.

summary of the essential equations in Greenspan's model see the Appendix.

Figure 1 shows the full growth history for both this model and the Greenspan model for one selected set of parameters $\sigma_\infty/\hat{\sigma} = 8.00$, $\sigma_i/\hat{\sigma} = 10^{-6}$ and $\gamma = 0.5$. The scaled time τ is taken relative to the beginning of the second phase.

These results show that there is a significant difference between the growth pattern predicted by this model and that predicted by the Greenspan model. In fact, it can be seen that in some cases the predicted radius of the necrotic core is larger than the predicted outer tumor radius in the Greenspan model. As pointed out by Deakin [5], the experimentally observed relative thickness [15] is more closely attained by the non-uniform consumption model than by the earlier Greenspan model, and the figure shows the growth pattern for a set of parameters which gives reasonable agreement with the experiments.

Finally, mention should be made of the use of these mathematical models to calculate parameters occurring in the models from experimental data. From the results shown here, this analysis of the data will be critically dependent on the model employed to carry out this interpretation.

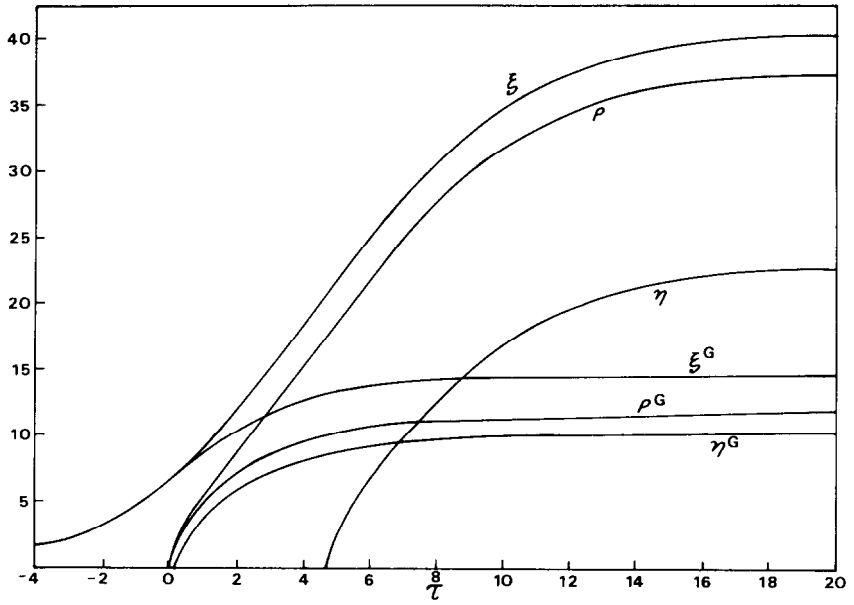

FIG. 1. Full growth patterns for this model and the Greenspan models for $\sigma_\infty/\hat{\sigma} = 8.00$, $\sigma_i/\hat{\sigma} = 10^{-6}$, $\gamma = 0.5$. The Greenspan values are denoted by a superscript G. The time τ is taken relative to the beginning of the second phase.

APPENDIX. SUMMARY OF THE GREENSPAN MODEL

In order to compare this model with the earlier model developed by Greenspan [9], the second of Greenspan's models in which there is "retardation due to nutrient deficiency" was recast in terms of the variables used in this work.

The first phase in Greenspan's model is the same as that considered in this model, with ξ being given by

$$\xi(\tau) = \xi(0)e^{\tau/3},$$

where ξ is the scaled outer radius and τ is the scaled time. This proceeds until $\xi = \xi_s$, where ξ_s is now given by

$$\xi_s = \left[6\left(\frac{\sigma_\infty}{\hat{\sigma}} - 1\right)\right]^{1/2}.$$

During phase II, the growth equation is

$$\xi^2 \frac{d\xi}{d\tau} = \tfrac{1}{3}(\xi^3 - \rho^3),$$

where ρ is the radius at which the concentration of oxygen, σ, is equal to $\hat{\sigma}$. In the model there is no growth for $r<\rho$, i.e., for $\sigma<\hat{\sigma}$. The radii ξ and ρ are related by

$$\frac{\sigma_\infty}{\hat{\sigma}} - 1 - \tfrac{1}{6}(\xi^2-\rho^2)=0.$$

This phase continues until the onset of necrosis, which occurs when $\xi=\xi_c$, where ξ_c is given by

$$\xi_c=\left[6\left(\frac{\sigma_\infty}{\hat{\sigma}}-\frac{\sigma_i}{\hat{\sigma}}\right)\right]^{1/2}.$$

The growth equation in phase III when $\xi>\xi_c$ is

$$\xi^2\frac{d\xi}{d\tau}=\tfrac{1}{3}(\xi^3-\rho^3)-\gamma\eta^3,$$

with ξ, ρ and η being related by the two equations

$$\frac{\sigma_\infty}{\hat{\sigma}} - 1 - \tfrac{1}{6}(\xi^2-\rho^2) - \frac{\eta^3}{3}\left(\frac{1}{\xi}-\frac{1}{\rho}\right)=0$$

and

$$\frac{\sigma_\infty}{\hat{\sigma}} - \frac{\sigma_i}{\hat{\sigma}} - \tfrac{1}{6}(\xi^2-\eta^2) - \frac{\eta^3}{3}\left(\frac{1}{\xi}-\frac{1}{\eta}\right)=0.$$

Although Greenspan gives a closed form for the solution of the growth equation for phase II, the procedure adopted here was to integrate the growth equation for phases II and III numerically, solving the appropriate equations for ρ in phase II and for ρ and η in phase III.

D. L. S. McElwain would like to express his appreciation of the hospitality shown to him by Professor B. W. Ninham of Department of Applied Mathematics, Research School of Physical Sciences, Australian National University.

REFERENCES

1 J. L. Bennington, Cellular kinetics of invasive squamous carcinoma of the human cervix, *Cancer Res.* **29**, 1082–1088 (1969).
2 J. W. Boag, Cell respiration as a function of oxygen tension, *Int. J. Radiat. Biol.* **18**, 475–478 (1970).
3 W. S. Bullough and J. U. R. Deol, The pattern of tumor growth, *Symp. Soc. Exp. Biol.* **XXV**, 255–275 (1971).

4 A. C. Burton, Rate of growth of solid tumors as a problem of diffusion, *Growth* **30**, 157–176 (1966).
5 A. S. Deakin, Model for the growth of an *in vitro* tumor, *Growth* **39**, 159–165 (1975).
6 R. E. Durand and R. M. Sutherland, Dependence of the radiation response of an *in vitro* tumor model on cell cycle effects, *Cancer Res.* **33**, 213–219 (1973).
7 J. Folkman and M. Hochberg, Self-regulation of growth in three dimensions, *J. Exp. Med.* **138**, 745–753 (1973).
8 G. Froese, The respiration of ascites tumor cells at low oxygen concentrations, *Biochem. Biophys. Acta* **57**, 509–519 (1962).
9 H. P. Greenspan, Models for the growth of a solid tumor by diffusion, *Stud. Appl. Math.* **52**, 317–340 (1972).
10 H. P. Greenspan, On the growth and stability of cell cultures and solid tumors, *J. Theor. Biol.* **56**, 229–242 (1976).
11 P. K. Lala, Personal communication to Tubiana, 1970 (see [17]).
12 P. K. Lala and H. M. Patt, Cytokinetic analysis of tumor growth, *Proc. Natl. Acad. Sci., U.S.A.* **56**, 1735–1742 (1966).
13 D. L. S. McElwain and L. E. Morris, Apoptosis as a volume loss mechanism in mathematical models of solid tumor growth, in preparation.
14 N. Rashevsky, *Mathematical Biophysics,* Vol. I, 3rd ed., Dover, New York, 1960.
15 R. M. Sutherland and R. E. Durand, Hypoxic cells in an *in vitro* tumor model, *Int. J. Radiat. Biol.* **23**, 235–246 (1973).
16 I. F. Tannock, The relation between cell proliferation and the vascular system in a transplanted mouse mammary tumor, *Br. J. Cancer* **22**, 258–273 (1968).
17 M. Tubiana, The kinetics of tumor cell proliferation and radiotheraphy, *Br. J. Radio.* **44**, 325–347 (1971).
18 R. Wette, I. N. Katz and E. Y. Rodin, Stochastic processes for solid tumor kinetics II. Diffusion-regulated growth, *Math. Biosci.* **21**, 311–338 (1974).